



Observation of the Huygens-principle growth mechanism in sputtered W/Si multilayers

To cite this article: T. Salditt *et al* 1996 *EPL* **36** 565

View the [article online](#) for updates and enhancements.

You may also like

- [The Huygens principle for flow around an arbitrary body in a viscous incompressible fluid](#)
Scott A Wymer, Akhlesh Lakhtakia and Renata S Engel
- [A simple method of demonstrating Huygens' principle in the classroom](#)
Stephen Hughes and Som Gurung
- [Fermat's principle, Huygens' principle, Hamilton's optics and sailing strategy](#)
J C Kimball and Harold Story

Observation of the Huygens-principle growth mechanism in sputtered W/Si multilayers

T. SALDITT¹, D. LOTT¹, T. H. METZGER¹, J. PEISL¹, R. FISCHER², J. ZWECK²
P. HØGHØJ³, O. SCHÄRPF³ and G. VIGNAUD⁴

¹ *Sektion Physik der Ludwig-Maximilians-Universität München
Geschwister-Scholl-Platz 1, D-80539 München, Germany*

² *Institut für Experimental Physik, Universität Regensburg
D-93040 Regensburg, Germany*

³ *Institut Laue Langevin, B.P.156, F-38043 Grenoble, France*

⁴ *ESRF - B.P. 220, F-38043 Grenoble, France*

(received 27 June 1996; accepted in final form 26 October 1996)

PACS. 05.40+j – Fluctuation phenomena, random processes, and Brownian motion.

PACS. 61.10-i – X-ray diffraction and scattering.

PACS. 68.55-a – Thin film growth, structure, and epitaxy..

Abstract. – We have investigated the interfacial roughness of a W/Si multilayer sputtered at high Ar gas pressure. The roughness exponents as determined from diffuse X-ray scattering agree well with the Huygens-principle growth model proposed by Tang, Alexander and Bruinsma (TAB). Simple microscopic explanations are given to account for the finding of Edwards-Wilkinson (EW) type growth at low Ar pressure and the TAB growth mechanism at high pressures, as well as for the absence of any scaling according to the Kardar-Parisi-Zhang (KPZ) equation.

In the last decade, much progress has been made in developing theories to describe the evolution of a rough interface during growth, mainly by the use of scale invariance or self-similarity [1]. However, the mapping of a theoretical model to a real growth process is non-trivial and must be supported by experimental evidence, *e.g.* by measuring the corresponding roughness exponents H and z , that describe the asymptotic scaling properties of the interface width w . For length scales smaller than the correlation length $r \ll \xi$, an algebraic increase $w \propto r^H$ is predicted, where the correlation length ξ grows with time according to $\xi \propto t^{1/z}$. Furthermore, the microscopic origins leading to a specific continuum growth equation should be elucidated. Due to its widespread application, the sputter deposition technique is a particularly interesting case. Recently, the interfacial roughness in an amorphous W/Si multilayer sputtered at low Ar gas pressure has been found to agree with the Edwards-Wilkinson (EW) model [2], where the evolution of the interface $h(\mathbf{r}, t)$ is described by a linear Langevin equation [1], [3],

$$\frac{\partial h(\mathbf{r}, t)}{\partial t} = \nu \nabla^2 h(\mathbf{r}, t) + \eta(\mathbf{r}, t). \quad (1)$$

ν is the relaxation coefficient and η a Gaussian white-noise term taking account of the random variations in the adatom flux. t denotes the time or the film thickness, if a Galilei transformation $t \rightarrow vt$ with a constant mean growth velocity v is applied. Assuming that the interface morphology remains in a metastable configuration, the model can also be applied to multilayers [4]. In this case, the correlations at different times translate into correlations between different interfaces, or *cross-correlations*. Accordingly, the interfacial roughness in multilayers can be characterized by height-height correlation functions $c_{ij}(r) := \langle h_i(\mathbf{r}'')h_j(\mathbf{r}') \rangle$, where i, j denote the indices of the different interfaces. For $i = j$, correlations in one interface are described (*self-correlation function*), while $i \neq j$ refers to correlations between different interfaces (*cross-correlation function*).

The solution of eq. (1) yields a logarithmic self-correlation function and an exponential cross-correlation function with a cross-correlation length $\xi_{\perp} \propto 1/(\nu q_{\parallel}^2)$. The experimental finding of this behavior was somewhat surprising, since it implies that the relaxation process is governed by the local curvature which is proportional to $\nu \nabla^2 h$. In the absence of an external field, surface diffusion cannot account for a relaxation of this type. On the other hand, the Gibbs-Thompson effect with a curvature-dependent chemical potential and the corresponding dynamics of condensation and evaporation cannot be expected to play a dominant role in sputtering either, where the substrate is usually not heated and where the system is driven far out of equilibrium by high flux rates. But, as discussed below, the sputtered adatoms impinging ballistically on the surface with high kinetic energy can resputter some of the more loosely bound atoms of the film back into the gas phase. We therefore conjecture that this site-dependent, local resublimation rate is governed by the local curvature on a mesoscopic scale.

However, the most general universality class for such a local growth model with non-conserved mass is that described by the Kardar-Parisi-Zhang (KPZ) equation [5], which one obtains by adding the nonlinear term $\nu_{\text{KPZ}}(\nabla h(\mathbf{x}, t))^2$ on the r.h.s. of the EW equation. If the coefficient ν_{KPZ} is small, there will first be a regime governed by the EW exponents before the crossover to the asymptotic KPZ behavior, which is given by $H \simeq 0.26$ and $z \simeq 1.6$ [1]. It is also well known that ν_{KPZ} is zero if all incoming particles are incorporated in a growing film with no voids, *i.e.* with homogeneous density. Furthermore, even if a finite fraction of particles is not incorporated (*e.g.*, as a result of resputtering), simple arguments show that ν_{KPZ} has to vanish, if the particle flux is perpendicular to the substrate. Thus the KPZ exponents will not be observed in high-quality samples. These usually exhibit a uniform density and are grown at the condition of low sputter pressure with a comparatively narrow angular distribution of ballistically impinging adatoms. However, the finite width of the distribution may become important at high flux, when an otherwise very small KPZ coefficient ν_{KPZ} can become relevant even at moderate time scales, since it is proportional to the average growth velocity v . Indeed, in the case of a crystalline NbN/AlN multilayer deposited on a sapphire substrate at 300°C at the relatively high flux ($v = 20 \text{ \AA/s}$), a KPZ-type behavior has been observed [6].

Furthermore, a distinct transition of the growth morphology is known to take place at high sputter pressure, when the sputtered atoms do no longer impinge ballistically on the substrate but are thermalized by collisions with sputter gas atoms [7]. In this case two major effects lead to a different growth mode: Firstly, the atoms loose kinetic energies by sometimes more than a factor 10, and secondly, they impinge isotropically. Cross-sectional transmission electron microscopy of such samples have revealed a very rough, columnar structure [8] that undergoes a coarsening process with time, *i.e.* small columns are absorbed by larger ones [8]. In the absence of a curvature-governed relaxation, surface diffusion may be the leading smoothing mechanism, which is, however, limited to rather small length scales in the case of amorphous films. For this regime, Tang, Alexander and Bruinsma (TAB) have proposed a model [9],

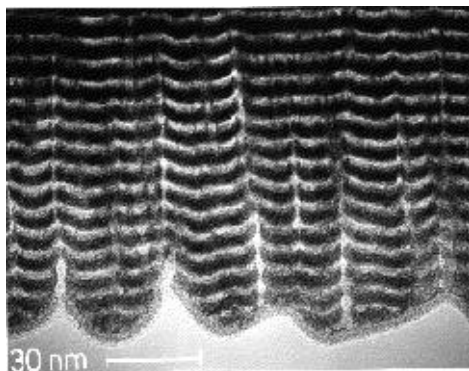


Fig. 1.

Fig. 1. – A TEM micrograph of the W (dark) and Si (light) layers near the top of the multilayer. The top bordering layer in the micrograph is not at the sample surface, but results from the sample thinning and preparation. A distinct network of columns and cusps is observed with column widths between 200 Å and 300 Å.

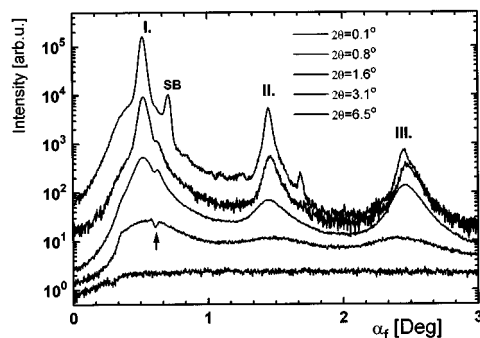


Fig. 2.

Fig. 2. – The intensity decay and increase in width of the multilayer Bragg sheets, as measured at angles of $2\theta = 0.1^\circ, 0.8^\circ, 1.6^\circ, 3.1^\circ$, and 6.5° (curves from top to bottom) out of the plane of incidence. The orders of the Bragg sheets are indicated by Roman numbers and the specular beam by SB. The curves at different 2θ have been normalized to the primary intensity (monitor counts). The arrow indicates a dynamic effect that cannot be described by simple kinematic theory.

where the broad tops of the columns evolve as if they were growing with a constant velocity along the local surface normal, analogously to the Huygens principle of geometrical optics. The columns are separated from each other by sharp cusps, that result from shadowing at an initial stage of growth.

Here we present a quantitative study of the columnar morphology encountered at high gas pressure, using diffuse X-ray scattering in a recently introduced setup [2], [10]. The values obtained for both roughness exponents H and z are well in agreement with the TAB model. The sample was taken from a series of W/Si multilayers grown on silicon by rf-sputtering at different Ar pressures and bias voltages at the substrate. Details of the deposition process, as well as the X-ray reflectivity and electron microscopy results are reported somewhere else [11]. The sample was electrically isolated and at ambient temperature. The pressure was at $p_{\text{Ar}} = 20 \cdot 10^{-3}$ mbar. A total of 60 bilayers was deposited, with periodicity $d = 80$ Å and sublayer ratio of about $d_{\text{Si}}/d_{\text{W}} = 5/3$. Both the W and Si layers were amorphous as evidenced by wide-angle X-ray scattering and TEM. The cross-sectional TEM micrographs obtained on a Philips CM300 microscope show a distinct columnar structure that starts to nucleate in about the first three-to-five multilayer periods, with a high degree of replication (conformality) to the layers on top. Furthermore, by comparing the interfaces near the bottom with those at the top, one can clearly observe a slow coarsening process of column widths, rather than a single wavelength selection by an interface instability. An enlarged image of the morphology in the top 15 bilayers is displayed in the TEM micrograph of fig. 1.

The diffuse X-ray scattering is analyzed in the kinematic framework using the structure factor as derived by Sinha and coworkers [12]. In a periodic multilayer the existence of cross-correlations gives rise to an intensity modulation along the perpendicular momentum transfer q_z (z -axis along the interface normal) with peaks at the positions of $q_z = n \cdot 2\pi/d$, the so-called diffuse Bragg sheets. The width of the Bragg sheet along q_z is determined by the number of interfaces that scatter in phase, *i.e.* by the vertical correlation length $\xi_{\perp}(q_{\parallel})$ for a

given fluctuation of wave vector q_{\parallel} [2]. Another quantity that is predicted by growth models and can be tested by the method is the average height-height self-correlation function of the interfacial roughness [1]. As can be shown from the X-ray structure factor in the approximation of small roughness, the self- and cross-correlations can be separated by integrating the diffuse intensity over one “Brillouin zone” $\Delta q_z = 2\pi/d$ in reciprocal space [2], [10]. In this case, one can treat the resulting expression by simple “one-interface” theory to obtain information on the average self-correlation function within the scattering depth Λ .

The experiment was performed at the *Troika* undulator beamline of the European synchrotron radiation facility ESRF and has been described in detail somewhere else [10]. As an example of the scattering data, in fig. 2 the intensity distribution along the exit angle α_f at constant angle of incidence $\alpha_i = 0.7^\circ$ is shown on a logarithmic scale at angles $2\theta = 0.1^\circ, 0.8^\circ, 1.6^\circ, 3.1^\circ$, and 6.5° (curves from top to bottom), where 2θ is the angle between the detector arm and the plane of incidence. The different curves are normalized to the primary intensity. At $2\theta = 0.1^\circ$ tails of the specular beam (SB) are still captured in the resolution volume of the detector. One can further observe the very strong first Bragg sheet (I.) and two more Bragg sheets (II., III.), which decay quickly in intensity with increasing 2θ . The increase in the full width at half-maximum (FWHM) of the Bragg sheets with 2θ reflects the decline of the cross-correlations for roughness fluctuations of smaller wavelength. However, for this sample the Bragg sheets persist up to relatively high values of 2θ (e.g., as compared to samples grown at low Ar pressure), indicating a large degree of conformality even at small wavelengths.

Figure 3 shows a double-logarithmic plot of the intensity distribution in the first Bragg sheet as a function of the momentum transfer parallel to the interfaces q_{\parallel} . The intensity has been integrated over the first Brillouin zone of the multilayer (circular data points). The intensity is nearly constant for $q_{\parallel} \leq 0.01 \text{ \AA}^{-1}$ and decays monotonically for more than 4 orders of magnitude before it levels off at $q_{\parallel} \geq 1 \text{ \AA}^{-1}$. The background level is indicated by the dotted line. It represents the contribution of amorphous scattering that is essentially constant over the considered range of reciprocal space and has to be subtracted from the data. The corresponding curve corrected for the amorphous background is shown with square data points. It exhibits a power law decay for $q_{\parallel} \geq 0.06 \text{ \AA}^{-1}$ with an exponent of $\gamma = 3.40$, as obtained from a least-square fit. In the approximation of small roughness the relationship $\gamma = 2 + 2H$ can be derived for the asymptotic algebraic decay of the structure factor. This is still valid in the present case, where a rms roughness σ in the range between 10 Å and 15 Å was determined by X-ray reflectivity [11]. Hence, a static roughness exponent of $H = 0.70$ is found for the interfaces that lie within the scattering depth $\Lambda \simeq 900 \text{ \AA}$, i.e. for about the top ten bilayers that are probed by the X-rays. The shoulder of the intensity distribution at $q_{\parallel} \simeq 0.04 \text{ \AA}^{-1}$ gives a lower bound for the correlation length $\xi \geq 150 \text{ \AA}$ in agreement with the TEM picture of fig. 1.

In fig. 4 the FWHM of the first Bragg sheet is shown as a function of q_{\parallel} . Due to the limited scattering depth, the width takes a constant value at $q_{\parallel} \leq 0.025 \text{ \AA}^{-1}$, firstly it increases slightly to a plateau around 0.04 \AA^{-1} and finally increases more rapidly for $q_{\parallel} \geq 0.06 \text{ \AA}^{-1}$. In this range a power law fit yields an exponent of $z = 1.37$ (solid line). Since the width of the Bragg sheets is inversely proportional to the vertical correlation length ξ_{\perp} , the relationship $\xi_{\perp} \propto q_{\parallel}^{1/z}$ can be deduced, from which the dynamic roughness exponent $z = 1.37$ is inferred [13]. This value is very close to $z = 4/3$ as predicted by TAB for the *late-stage coarsening* of the columnar morphology. Correspondingly, the value H determined in the experiment is close to the value $2 - z = 0.67$ as expected from a general scaling relation $2 - z = H$ [1], that has been shown to be valid also in the TAB model [9]. If one estimates the experimental errors to about

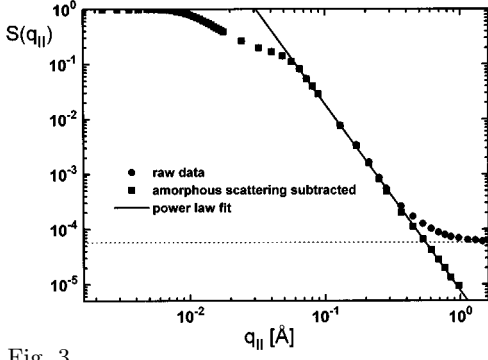


Fig. 3.

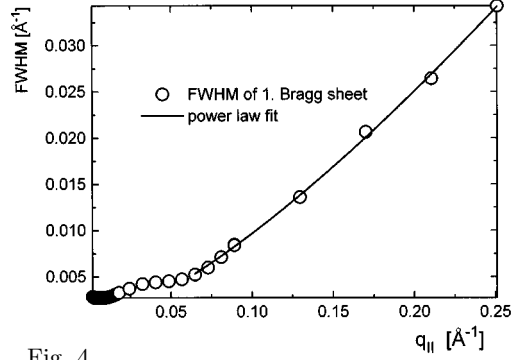


Fig. 4.

Fig. 3. – The decay of the intensity integrated over the first Bragg sheet as a function of $q_{||}$ on a double-logarithmic scale. The squared data points are obtained by subtraction of the amorphous scattering contribution (dotted line) from the original data points (circular points). The solid line corresponds to a power law decay with an exponent $\gamma = 3.4$.

Fig. 4. – The increase of the FWHM along q_z (Bragg sheet I.) as a function of $q_{||}$. The solid line corresponds to a power law increase with an exponent of $z = 1.37$.

$\Delta H = 0.05$ and $\Delta z = 0.1$, the experimental result clearly confirms these predictions.

In contrast to the KPZ equation, there is no curvature-dependent relaxation term present in the model of TAB, so that large interface gradients will build up and lead to shadowing effects. As a consequence, the interface becomes unstable and will evolve to a columnar structure at an early stage of growth, similar to other deterministic models of columnar growth [14]. However, in a later regime, the so-called *late-stage coarsening*, shot noise leading to fluctuations in the column heights may become important and fix the roughness exponents to the values cited above. According to theory, the critical film thickness d^* for the crossover to late-stage coarsening is proportional to the square of the surface diffusion length l . For amorphous films, the surface mobility and hence l is typically much smaller than for crystalline films. It can be estimated from the relation $l \simeq (a^{3/2}/\xi^2)d^{3/2}$ [9] with a total film thickness of $d = 4800$ Å, a correlation length of about 300 Å, and an atomic distance a to be around $l \simeq 20$ Å. Hence, *late-stage coarsening* may set in after the first few layers.

The studies of interfacial roughness below and above the thermalization threshold indicate the crucial role of resputtering as the major relaxation mechanism responsible for the good quality of samples grown at low sputter pressure p_{Ar} . This is possible, since the energy distribution of sputtered atoms as they leave the target has a peak at about half the binding energy E_b , and then falls off like $1/E^2$ with a cut-off at $4m_1m_2/(m_1 + m_2)^2$, where m_1 and m_2 are the masses of the sputter and sputtered atoms, respectively [15]. The energy difference between the ejected particles and the atoms of the sputter gas (*e.g.*, argon) then decays exponentially with the number of collisions n , like $\Delta E = \exp[n \ln(E_f/E_i)]$, where E_f/E_i is the ratio of energies after and before a collision, and $n = dp\sigma/k_B T_{gas}$. For typical values of $d = 5$ cm, $\sigma = 10^{-19}$ m², and $T_{gas} = 500$ K, the average number of collisions is nearly two at $p_{Ar} = 20 \cdot 10^{-3}$ mbar, and zero for the reference samples grown at $3.3 \cdot 10^{-3}$ mbar [11]. The energy loss by elastic collisions would therefore be 97% and 59% for the Si and W atoms, respectively. While an adatom impinging on the growth front with an energy of $0.5 E_b$ has a finite probability to resputter surface atoms that are less well coordinated, *i.e.* in surface regions of positive curvature, this is clearly ruled out after yet two collisions.

In summary, we obtain the following picture: at low gas pressures a resputtering of surface

atoms by the highly energetic adatoms gives rise to an EW-type relaxation. In this regime, the nonlinear KPZ behavior is not observed, probably as a result of a relatively narrow angular distribution of adatoms impinging on the substrate. At high gas pressure a smaller mean free path leads to an isotropic distribution of incident angles, in favor of a stronger KPZ term. However, at the same time, the thermalization of atoms due to collisions with gas atoms suppresses the curvature-governed (EW/KPZ-type) relaxation. Thus a transition from EW to TAB instead of KPZ behavior is observed. These conclusions could be tested in a future experiment, where the adatoms impinge both isotropically and with high energy. In this case the KPZ exponents should appear.

This work was supported by the Bundesministerium für Forschung und Technologie under contract No. 055WMAXI5. We thank G. GRÜBEL, J. LEGRAND, and D. ABERNATHY for their excellent support at the *Troika* beamline of the ESRF.

REFERENCES

- [1] BARABÁSI A. L. and STANLEY H. E., *Fractal Concepts in Surface Growth* (Cambridge University Press) 1995, and references therein.
- [2] SALDITT T., METZGER T. H. and PEISL J., *Phys. Rev. Lett.*, **73** (1994) 2228.
- [3] EDWARDS S. F. and WILKINSON D. R., *Proc. R. Soc. London, Ser. A*, **381** (1982) 17.
- [4] STEARNS D. G., *Appl. Phys. Lett.*, **62** (1993) 1745.
- [5] KARDAR M., PARISI G. and ZHANG Y. C., *Phys. Rev. Lett.*, **56** (1986) 869.
- [6] MILLER D. J., GRAY K. E., KAMPWIRTH R. T. and MURDUCK J. M., *Europhys. Lett.*, **19** (1992) 27.
- [7] FULLERTON E. E. *et al.*, *Phys. Rev. B*, **48** (1993) 17432.
- [8] MESSIER R. and YEHOUDA J. E., *J. Appl. Phys.*, **58** (1985) 3739.
- [9] TANG C., ALEXANDER S. and BRUINSMA R., *Phys. Rev. Lett.*, **64** (1990) 772.
- [10] SALDITT T. *et al.*, *Physica B*, **221** (1996) 13.
- [11] SALDITT T. *et al.*, *Phys. Rev. B*, **54** (1996) 5860.
- [12] SINHA S. K., *J. Phys. III*, **4** (1994) 1543
- [13] KARDAR M., private communication.
- [14] BALES G. S. and ZANGWILL A., *Phys. Rev. Lett.*, **63** (1989) 692, and references therein.
- [15] MEYER K., SCHULLER I. K. and FALCO C. M., *J. Appl. Phys.*, **52** (1981) 5803, and references therein.